

Thermal, mechanical and viscoelastic properties of citric acid-crosslinked starch/cellulose composite foams

M. M. Hassan^{*,1,4}, N. Tucker^{2,4,†}, Marie Joo Le Guen^{3,4}

¹ Bioproduct and Fibre Technology Team, AgResearch Limited, 1365 Springs Road, Lincoln 7647, Canterbury, New Zealand.

² Bioresources Engineering and Chemistry Group, The New Zealand Institute for Plant & Food Research, Gerald Street, Lincoln, Canterbury 7608, New Zealand.

³ Biopolymers and Chemicals Team, Scion, 49 Sala Street, Rotorua 3010, New Zealand.

⁴ Biopolymer Network (BPN), 49 Sala Street, Rotorua 3010, New Zealand.

Abstract:

In this work, biodegradable starch/cellulose composite foams were fabricated at 220 °C by compression moulding gelatinised starch containing cellulose fibres as a reinforcing agent and citric acid as a cross-linking agent. It was found that the stiffness, tensile strength, flexural strength, and hydrophobicity of the starch/cellulose composite foams increased, and

* Corresponding author. Tel.: +64-3-321-8755, fax: +64-3-321-8811

Email: mahbubul.hassan@agresearch.co.nz (M. M. Hassan)

† Current address: University of Lincoln, School of Engineering, Brayford Pool, Lincoln, LN6 7TS, United Kingdom.

water absorption capacity decreased with an increase in the concentration of citric acid. The tensile strength increased from 1.76 MPa for 0% citric acid to 2.25 MPa for the starch/cellulose composite foam crosslinked with 5% (w/w) citric acid. Similarly, the flexural modulus also increased from 445 MPa to 601.1 MPa, and the flexural strength from 3.76 MPa to 7.61 MPa, for the composite foam crosslinked with 5% (w/w) citric acid. The crosslinked composite foams showed better thermal stability compared to the non-crosslinked composite foam. The resulting composite foams could be used as a biodegradable alternative to expanded polystyrene packaging.

Key-words: Biocomposites; starch/cellulose foam; cross-linking; viscoelastic properties; moisture absorption; flexural properties

1. Introduction

Municipal waste comprises a mixture of materials including those of biological origin (such as paper and timber), plastics, and metals; some of which are potentially hazardous. A study carried out by the US Environmental Protection Agency reported that in 2015, the total municipal solid waste produced in the USA was 262.4 million tons, of which 34.8 million tons were a plastic waste (Report No. EPA530-F-18-004, 2018). These wastes can be generated throughout a material's life-cycle - including extraction, manufacturing, transportation, and consumption. The thermoplastic foams are used as packaging as well as in household applications, such as furniture, and insulation. These foams are very popular as packaging not only because of their ultra-low density, but also they exhibit good thermal insulation properties and readily absorb impact to protect packaged goods from transit damage. The most popular foam packaging is made of either expanded polystyrene (EPS) or

synthetic polyurethane; neither of them is biodegradable. Currently, only a small portion of the used packaging is recycled and most of the plastic foam packaging materials end up in a landfill.

Starch is highly biodegradable, renewable, inexpensive, and also abundantly available being extracted from potato, rice, wheat, corn, tapioca, cassava, and other crops (Bergel et al, 2018; Aygün et al., 2017; Cruz-Tirado et al., 2019). At high temperatures and pressures, starch loses its crystallinity and becomes thermoplastic, but the films cast from this material are brittle, which limits their applications. To toughen the material, plasticisers including glycerol and water are added, which enable it to be processed by common thermoplastic processing routes, such as injection moulding (Meng et al., 2019; Stepto, 2006; Swanson et al., 1993). Starch foams have thermal insulation properties comparable to commercial fossil-fuel derived polymer foam containers (Bergel, 20184). However, current starch foams have significant shortcomings compared to polystyrene-based synthetic foams. Foams produced from starches exhibit very low mechanical strength and poor water barrier properties, severely limiting their applications (Dos Santos et al., 2018). The mechanical behaviour of thermoplastic starch foams changes with relative humidity. In wet or humid conditions, the starch-based foams lose their strength and structural integrity. Starches with high amylose content produce stronger foam than the foam made from starch-containing low amylose content but at the expense of flexibility (Noorbakhsh-Soltani et al., 2018). Conversely, starch with high amylopectin content produces light-weight foams but at the expense of strength (Glenn et al., 2001).

To increase the strength and moisture barrier properties of starch foams, the addition of hydrophobic synthetic polymers, such as cryogenic milled PLA powder (Hassan et al., 2019), polypropylene (Xu et al., 2016) and polybutylene succinate (Phiriyawirut et al., 2016), have been investigated. The addition of PLA to cellulose reinforced starch foam has shown

enhanced moisture barrier properties and increased flexural strength, flexural modulus and tensile strength (Hassan et al., 2019). A range of cellulosic fibrous materials including sugarcane bagasse fibres (Dos Santos et al., 2018), flax fibres (Romero-Bastida et al., 2016), date palm fibres (Ibrahim et al., 2017), jute fibres (Wang et al., 2017), cellulose nanocrystals (Ali et al., 2018), microcrystalline cellulose (Chen et al., 2017), sugar palm fibres (Edhirej et al., 2017), and cellulose nano-whiskers (Liu et al., 2017) have been investigated as a reinforcing agent with considerable improvement in increasing the strength of starch foam. The addition of nano-clay (Romero-Bastida et al., 2016), β -glucan (Sagnelli et al., 2017), and wheat gluten (Muneer et al., 2015) to starch also improves its strength and water barrier properties.

Starch has abundant hydrophilic hydroxyl groups, and therefore composites made from it have poor moisture barrier properties. Acylation and hydroxypropylation have been investigated to convert hydrophilic hydroxyl groups to hydrophobic groups to enhance moisture barrier properties (Shaikh et al., 2019; Zamudio-Flores et al., 2010). The modification of hydroxyl groups of starch with hydrophobic octenyl- or alkenyl-substituted succinic acid anhydride marginally improved the water vapour permeability, which is lower than the water vapour permeability achieved with the addition of hydroxypropylated starch to cellulose (Jansson et al., 2005). The hydrophilicity of starch can be substantially decreased by blocking some of its hydroxyl groups by crosslinking. Citric acid (Zhou et al., 2016; Seligra et al., 2016), glutaraldehyde (Gonenc & Us, 2019), and malonic acid (Ghosh & Netravali, 2012) have been investigated for the crosslinking of hydroxyl groups of starch and cellulose.

In this work, we added cellulose powder and citric acid to starch to reinforce and enhance the moisture barrier properties of starch and cellulose composite foam. The starch/cellulose composite foams were made by high-temperature compression moulding and investigated the effect of citric acid crosslinking on the thermal stability, mechanical and viscoelastic

properties, and moisture barrier properties. To the best of our knowledge, no published literature reported the viscoelastic, thermal and flexural properties of such starch/cellulose composite foams crosslinked with citric acid.

2. Experimental section

2.1. Materials

Potato starch with an average granule size of 96 μm was donated by Earthpac Limited (New Zealand). This potato starch contains 28.6% amylose and 71.4% amylopectin. Microcrystalline cellulose powder (100% cellulose, degree of polymerisation = approx. 220) derived from wood pulp with a length between 500 to 800 μm and a width between 15 to 34 μm , was purchased from Innventia AB (Stockholm, Sweden). Carnauba wax was also provided by Earthpac Ltd. Analytical reagent-grade citric acid and sodium hypophosphite were purchased from Sigma-Aldrich Chemicals (Switzerland).

2.2. Preparation of crosslinked starch/cellulose composite foams

The plate-shaped composite foam test articles were made by a one-step hot compression moulding of a predetermined amount of moistened mixture of starch, cellulose, carnauba wax and various weight (%) of citric acid. Carnauba wax was added as an internal mould release

agent as well as a hydrophobicising agent. In the manufacturing of starch/cellulose composites, the weight (%) of starch, carnauba wax, and cellulose was kept fixed, but the weight (%) of citric acid was varied. A small quantity of water was added to the starch/cellulose/wax mixture to facilitate gelatinisation of starch through disruption of its structure by steam explosion.

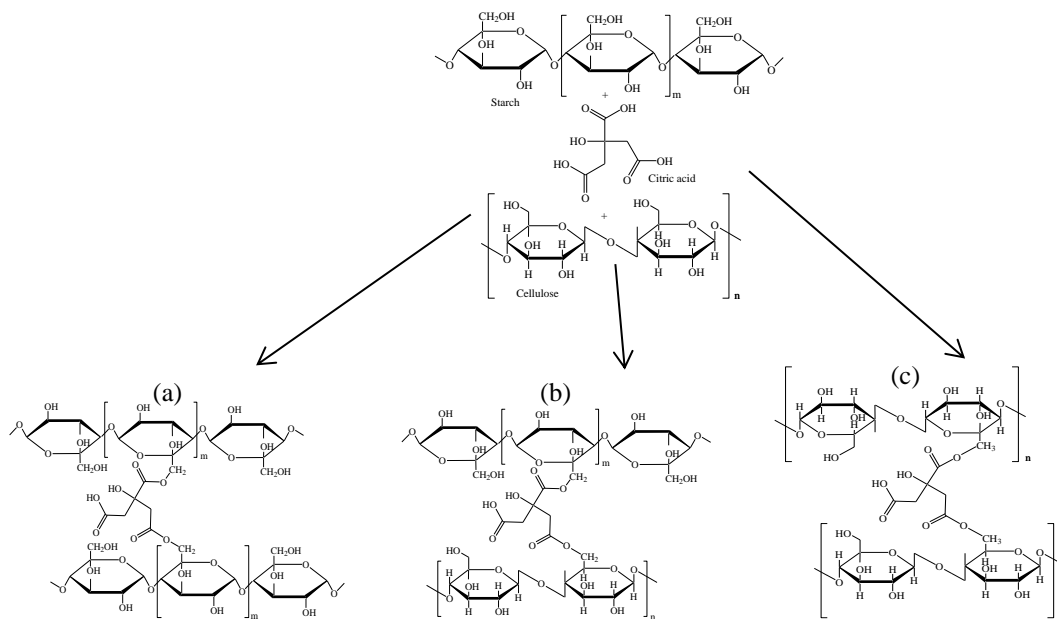


Fig. 1. The mechanism of crosslinking of starch (a), cellulose (c), and also crosslinking between starch and cellulose (b) with citric acid.

For the fabrication of citric acid crosslinked starch cellulose composites, 146.0 g starch, 48.8 g cellulose powder, and 5.2 g Carnauba wax were mixed together by using a food mixer at a slow speed so that powders do not go out of the mixing bowl. Then 1, 3, 5, 6, and 7% citric acid (of the combined weight of starch and cellulose), and sodium hypophosphite (50% of the weight of citric acid) were dissolved in 122.4 ml water, which was gradually added to the starch/cellulose/carnauba wax mixture with continuous slow stirring (200 rpm). For the

control sample, only water was added to the starch, cellulose and carnauba wax mixture. The final moistened mixture was mixed at high speed (1500 rpm) for 60 s. A small amount of the mixture (85 g) was compression moulded at a pressure of 2 MPa in a plate-shaped mould at 220 °C for 60 s and 2.20 mm thick composite foam plates were prepared.

The mechanism of crosslinking of starch and cellulose is shown in Fig. 1. The OH group at position C6 of starch and cellulose is the most reactive because of its lower steric hindrance compared to other OH groups at C2 and C3 positions (Ramos et al., 2005), and therefore crosslinking takes place predominantly between OH groups at the C6 position of various molecular chains of starch and cellulose. Citric acid not only causes self-crosslinking of starch and cellulose by reacting with hydroxyl groups of two macromolecular chains of each polymer but also forms crosslinking between hydroxyl groups of macromolecular chains of starch and cellulose through the formation of ester bonds (Demitri et al., 2008; Zhou et al., 2016). During high-temperature compression moulding in the presence of a plasticiser, the starch powders are quickly gelatinised and make a viscous liquid (Nashed et al., 2003). Water and other volatiles are evaporated and dry foam plates were produced. The foam composite samples were stored at 20 ± 2 °C and $65\pm 2\%$ relative humidity.

2.3. Thermal stability

Thermo-gravimetric analysis (TGA) was carried out from room temperature to 500 °C at a heating rate of 5 °C/min by using a thermogravimetric analyser (Model 550, TA Instruments Inc., New Castle, USA) under nitrogen. At least three samples were tested and the specimen TGA curves were shown.

2.4. Mechanical properties

The effect of crosslinking by increasing the concentration of citric acid on the tensile properties of the starch/cellulose composite foams was studied. Specimens of 15.0×70 mm in dimension crosslinked with 1, 3, and 5% (w/w) citric acid were cut from the compression moulded composite foams and preconditioned at least 48 h at 20 ± 2 °C and $65 \pm 2\%$ relative humidity (Hassan et al., 2019). The tensile strength and elongation properties of the composite foams were also measured at 20 ± 2 °C and $65 \pm 2\%$ relative humidity by using an Instron Universal Tensile Testing machine according to a published literature but at a crosshead speed of 20 mm/min and a gauge length of 30 mm (Preechawong et al., 2005). Flexural tests were carried out according to *ASTM Test Method D 790-03* using a 3-point flexural test rig attached to an Instron Universal Tensile Testing machine at a crosshead speed of 2 mm/min using a span length of 34.4 mm at the same atmospheric conditions the tensile measurements were carried out. For the flexural measurements, the sample size was $60 \times 20 \times 2.2$ mm and samples were preconditioned at the standard atmospheric conditions for 48 h prior to the test. In this method, the test specimens were supported at both ends and force was applied from the top in the middle of the specimen. From the peak force to deform the specimen, the flexural strength and flexural modulus were calculated. The vertical displacement was measured at the centre of the span using an LVDT displacement transducer. The flexural strength was calculated according to the following formula:

$$\sigma = \frac{3 \times F \times L}{2bh} \quad [2]$$

The flexural modulus was calculated according to the following equation:

$$E_{bend} = \frac{L^3 \times F}{4bh^3d} \quad [3]$$

where, L = span length, F = force, b = sample width, h = sample thickness and d = deflection. For each sample, at least 10 tests were carried out and the averages are reported here.

2.5. Dynamic mechanical thermal analysis

For the dynamic mechanical thermal analysis (DMTA), samples of 15 × 56 × 2.2 mm size were cut from various starch/cellulose composite foams (crosslinked and non-crosslinked control). DMTA experiments were carried out in 3-point flexural mode using a dynamic mechanical analyser (Model RSA-G2, TA Instruments, New Castle, USA). The dynamic measurements were recorded during a heat ramp starting from $T = 25\text{ }^{\circ}\text{C}$ to $200\text{ }^{\circ}\text{C}$ at a rate of $5\text{ }^{\circ}\text{C}/\text{min}$ at a frequency of 1 Hz and 0.1% strain. The storage modulus (E'), loss modulus (E''), and loss factor ($\tan \delta$) of the samples were measured in triplicate and examples of a typical curve are presented.

2.6 Measurement of colour

A reflectance spectrophotometer (Color eye 40/0, Mahlo GmbH, Germany) was used to measure the $CIE L^*a^*b^*$ values of the starch/cellulose composite under D65 illuminant and 10° observer. The whiteness index was deduced according to the following equation:

$$Whiteness\ index = 100 - [(100 - L^*)^2 + (a^*)^2 + (b^*)^2]^{0.5} \quad [1]$$

2.7. Surface characterisations

The contact angle was measured in dynamic mode by using a KSV CAM 100 Contact Angle Measurement Apparatus (KSV Instruments, Finland). For each sample, the contact angle was measured at 5 places on both sides of the droplet. The average contact angle is reported here. The contact angles were quantified by using the Young-Laplace equation. The first measurement was taken immediately after placing the water droplet and the successive measurements were taken at 120 s interval until 480 s.

The neat and the cracked surface of composite foams were characterised by scanning the surface without any conductive coating using backscattered mode on a Hitachi scanning electron microscope (Model: TM3030Plus, Hitachi Corporation, Japan) at an accelerating voltage of 15 kV.

The infrared (IR) spectra of the composite foam surfaces were recorded using a PerkinElmer FTIR (Model: System 2000, PerkinElmer Corporation, USA) equipped with an attenuated total reflectance (ATR) attachment using a Zn/Se ATR crystal from 650 to 4000 cm^{-1} . The samples were placed flat on the upper side of the crystal. Good fibre to crystal contact was ensured by applying 50 N force using a calibrated torque wrench. 64 scans were carried out for each sample.

2.8. Water absorption

The water absorption capacity of starch/cellulose composites cross-linked with various concentrations of citric acid was measured according to *ASTM Test Method D570: Standard*

Test Method for Water Absorption of Plastics at room temperature. $40 \times 40 \times 2.2$ mm size samples were cut from the crosslinked composite foams and each sample was immersed in a water tank containing 100 ml distilled water. After which, they were removed from the tank after 10, 20, 30, 60, and 240 min, water adhered on the surface was removed by a tissue paper and the dried samples weighed. Finally, the water uptake was calculated as the mass difference, expressed as a percentage.

2.9. Statistical analysis

All tests were performed 10 times except otherwise stated. Analysis of variance (ANOVA) was used to test the statistical significance with SPSS (v. 20) statistical software. Bonferroni post hoc multiple-range test was performed and pair-wise comparison was made between control samples and composites crosslinked with various concentrations of citric acid, and also between composites crosslinked with different concentrations of citric acid. A p -value < 0.05 was considered statistically significant (Jiang et al., 2019).

3. Results and discussion

3.1. Colour of the crosslinked starch/cellulose composites

It is necessary to assess the colour of the composites not only for an aesthetic reason but also change in colour may suggest whether the composites had undergone any degradation. All the starch/cellulose composites crosslinked with 1, 3, 5, 6 and 7% (w/w) citric acid had

no visible cracks or holes and the surface of the produced composite materials was quite smooth as evident from optical micrographs presented in Fig. 2. The colour of the crosslinked composites progressively changed compared to the control with an increase in the citric acid concentration. The *CIE L*a*b** values and whiteness index of a control starch/cellulose composite and citric acid crosslinked starch/cellulose composites are presented in Table S1 (Supplementary Material). The increase in the value of L^* suggests the colour is lighter and the decrease indicates the colour is darker. For the crosslinked composites, the value of L^* and whiteness index decreased with an increase in the concentration of citric acid suggesting that the colour of the composite foams became darker with an increase in the citric acid concentration. The value of L^* of the control composite material was 93.54, which marginally increased in the case of starch/cellulose composites crosslinked with 1% citric acid. However, a further increase in the citric acid concentration to 7% resulted in a decrease of the L^* value to 89.53. Similarly, the value of a^* and b^* increased with an increase in the citric acid concentration. The value of a^* increased from 1.15 observed for the control composite to 2.55 for the composite crosslinked with 7% citric acid suggesting a considerable increase in redness of the composites. Similarly, the value of b^* also increased from 13.97 for the control to 17.55 for the composites crosslinked with 7% (w/w) citric acid, indicating the increase of yellowness of the composites with an increase in the citric acid concentration. The increase in the yellowness suggests that starch and cellulose might have undergone some levels of thermal degradation during crosslinking at 220 °C (Soares et al., 2001; Liu et al., 2013).





Fig. 2. Visual appearance of starch/cellulose foam composite plates crosslinked with various concentrations of citric acid.

3.2. Tensile strength

The tensile strength and elongation to failure of the composites were measured to quantify the influence of crosslinking on mechanical properties. Table 1 shows the tensile strength, strength to failure and elongation at break of starch/cellulose composites crosslinked with various concentrations of citric acid. The crosslinking with citric acid had a positive effect on the tensile strength and strength to failure (breaking strength) up to the citric acid concentration of 5% (w/w) as both tensile strength and breaking strength increased by almost 30% compared to the control composite foam but beyond that level, the tensile strength decreased.

Table 1

Mechanical properties of starch/cellulose composites crosslinked with various concentrations of citric acid (standard deviations are provided in parenthesis, and detailed statistical results are provided in ‘Supplementary Material’).

Citric acid concentrations (%)	Tensile strength (MPa)	Elongation at peak (%)
--------------------------------	------------------------	------------------------

0	1.76 (0.03)	1.97 (0.04)
1	1.82 (0.02)*	1.67 (0.03)*
3	2.08 (0.06)*	1.37 (0.04)*
5	2.25 (0.05)*	1.27 (0.02)*
7	1.98 (0.04)*	1.20 (0.03)*

* *p*-value less than 0.05

The control composite foam showed tensile strength of 1.76 MPa, which increased to 2.25 MPa for the starch/cellulose foam crosslinked with 5% (w/w) citric acid. The increase in tensile strength achieved for up to 3% (w/w) citric acid provided a relatively low increase compared to the increase achieved for the 5% citric acid. The results obtained suggest that the degree of crosslinking between molecular chains of starch, cellulose and also starch and cellulose increased with an increase in the concentration of citric acid, but beyond the 5% (w/w), probably induced acid catalysed hydrolytic degradation of both cellulose and starch. Reddy and Yang also observed a similar trend in increasing the citric acid concentration on the tensile strength of cross-linked corn starch films (Reddy and Yang, 2010). Conversely, the increase in citric acid concentration resulted in a decrease in the elongation properties of the composite foams. The increase in the degree of crosslinking decreased the mobility of the starch and cellulose chains, resulting in a decrease in the elongation of the composite foams. Mi et al. found that in the case of crosslinking of chitosan with genipin, the increase in the crosslinking decreased the elongation at break of chitosan (Mi et al., 2005). Similarly, other researchers also observed that the elongation at break decreased with an increase in the crosslinking in the case of crosslinked latex (Pinenq and Winnik, 2000).

3.3. Flexural properties

The effect of crosslinking on the flexural strength and stiffness of the starch/cellulose composite foams were measured using a 3-point flexural test, and the results are shown in Fig. 3 (top). The citric acid crosslinking had a positive effect on the flexural strength of the starch/cellulose composites. The beneficial effect on the flexural strength was seen for the concentration of citric acid up to 5% (w/w) but a further increase in the concentration resulted in a gradual decrease in the flexural strength, consistent with the tensile properties. The lowest flexural strength (3.76 MPa) was observed for the control starch/cellulose foam. However, all the crosslinked composite foams showed higher flexural strength compared to the control foam. The flexural strength increased with the increased citric acid concentration and reached to the highest (7.61 MPa) for the starch/cellulose foam crosslinked with 5% citric acid, which is more than double of the flexural strength exhibited by the control composite foam. Increasing the concentration of the citric acid above 5% (w/w) reduced the flexural strength. The starch/cellulose composite crosslinked with 7% showed lower flexural strength (4.69 MPa) compared to composites crosslinked with 5% citric acid. Therefore, 5% (w/w) is the optimum concentration of cross-linker to achieve the highest flexural strength. The increase in flexural strength of starch/cellulose composites with the increase in the concentration of citric acid up to 5% (w/w) suggest that the degree of crosslinking between macromolecular chains of starch, cellulose, and starch/cellulose increased with the increase in citric acid concentration resulting in increased flexural strength of the composite foams.

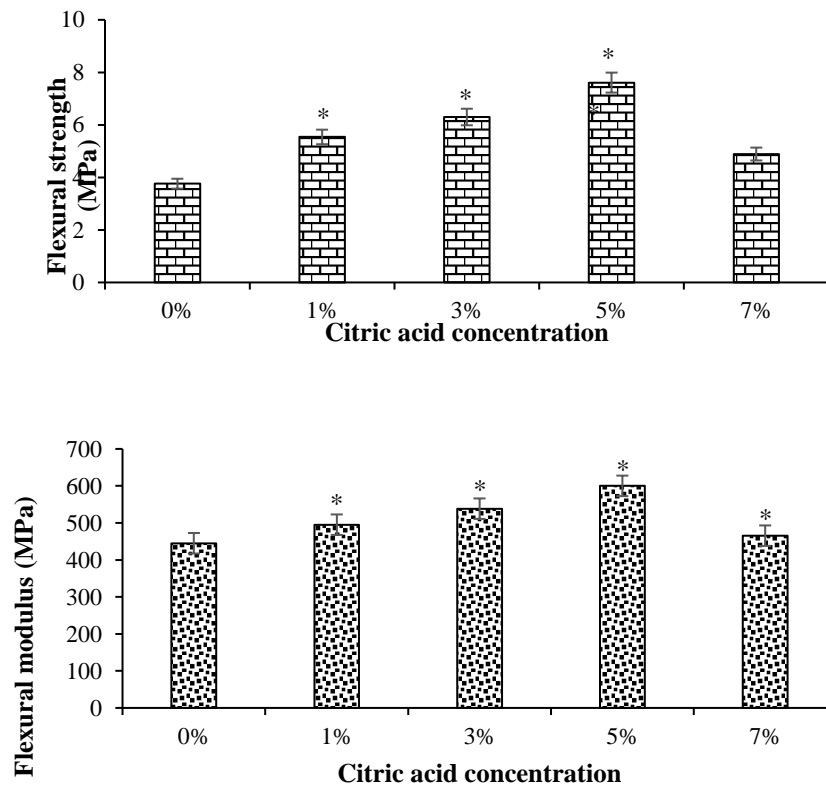


Fig. 3. Effect of increase of cross-linker concentration on the flexural strength (top) and flexural modulus (bottom) of starch/cellulose composite foams measured at 20 ± 2 °C and $65\pm 2\%$ relative humidity (error bars are based on standard deviation). Detailed statistical results are provided in ‘Supplementary Material’.

Fig. 3 (bottom) shows the flexural moduli of starch/cellulose composite foams crosslinked with varying amounts of citric acid. The flexural modulus exhibited by the control starch/cellulose foam composite was 445.1 MPa, which increased to 600.0 MPa for starch/cellulose composites crosslinked with 5% (w/w) citric acid; an increase of about 35% in stiffness. The flexural moduli data are consistent with the flexural strength data and a decrease in flexural moduli was observed for the citric acid concentration beyond 5% (w/w).

Preechawong et al. reported that at 65% relative humidity, tapioca starch foam exhibited a flexural strength of approximately 0.48 MPa (Preechawong et al., 2005). Although we used shorter span length and slightly higher crosshead speed in the assessment of flexural properties, the control potato starch/cellulose composite described here exhibited flexural strength of 3.8 MPa, considerably higher than the tapioca starch foam reported by Preechawong et al. The addition of cellulose to starch reinforced the produced starch foam, thereby increasing the flexural strength. The crosslinking with citric acid increased the flexural strength of the starch/cellulose composite by almost 100% compared to the flexural strength shown by the control starch/cellulose composite. As the increase in the concentration of citric acid beyond 5% (w/w) provided a decrease in flexural strength and modulus, for further experiments the concentration of citric acid was limited to 5% (w/w).

3.4. Dynamic mechanical thermal analysis (DMTA)

The effect of the crosslinking of the starch/cellulose composite foams on the stiffness and viscoelastic properties was assessed by dynamic mechanical thermal analysis. Fig. 4 (top) shows the representative storage moduli (E') and loss moduli (E'') curves from room temperature to 200 °C of starch/cellulose composite foams crosslinked with 1, 3, and 5% (w/w) citric acid. The storage modulus (E') of the starch/cellulose composite foam increased with an increase in the concentration of citric acid up to 5% (w/w) but a further increase in the concentration resulted in a decrease in the storage modulus. For all the samples, the storage modulus decreased with an increase in the temperature indicating a progressive reduction of stiffness with the increased temperature. The control starch/cellulose composite foam showed the lowest stiffness at all temperatures and the starch/cellulose composite foam

crosslinked with 5% (w/w) citric acid showed the highest storage modulus (E'), which is consistent with the flexural moduli. At 30 °C, the storage modulus of the control starch/cellulose composite foam was 0.82 GPa, which increased to 0.87 GPa for the composite foam crosslinked with 1% citric acid. The increase in the applied concentration of citric acid to 3% and 5% increased the storage modulus (E') to 0.83 and 1.03 GPa respectively. The results indicate that the increase in crosslinking increased the stiffness of the starch/cellulose composite foams. Compared to this, storage moduli of the control composite foam were 0.62 and 0.46 GPa at 86 and 200 °C respectively. The corresponding values for the starch/cellulose composite foam crosslinked with 1, 3, and 5% (w/w) citric acid were 0.70 and 0.52, 0.76 and 0.51, and 0.85 and 0.69 GPa respectively. These results indicated that 5% (w/w) citric acid provided the highest stiffness for the starch/cellulose composite foam.

The loss modulus data also showed a trend similar to the storage modulus data; i.e. the loss modulus of the composite foam increased with an increase in the concentration of citric acid. The non-crosslinked starch cellulose composite showed the lowest loss modulus and the composite foam crosslinked with 5% (w/w) citric acid showed the highest loss modulus. All the samples showed very similar loss moduli at temperatures above 170 °C.

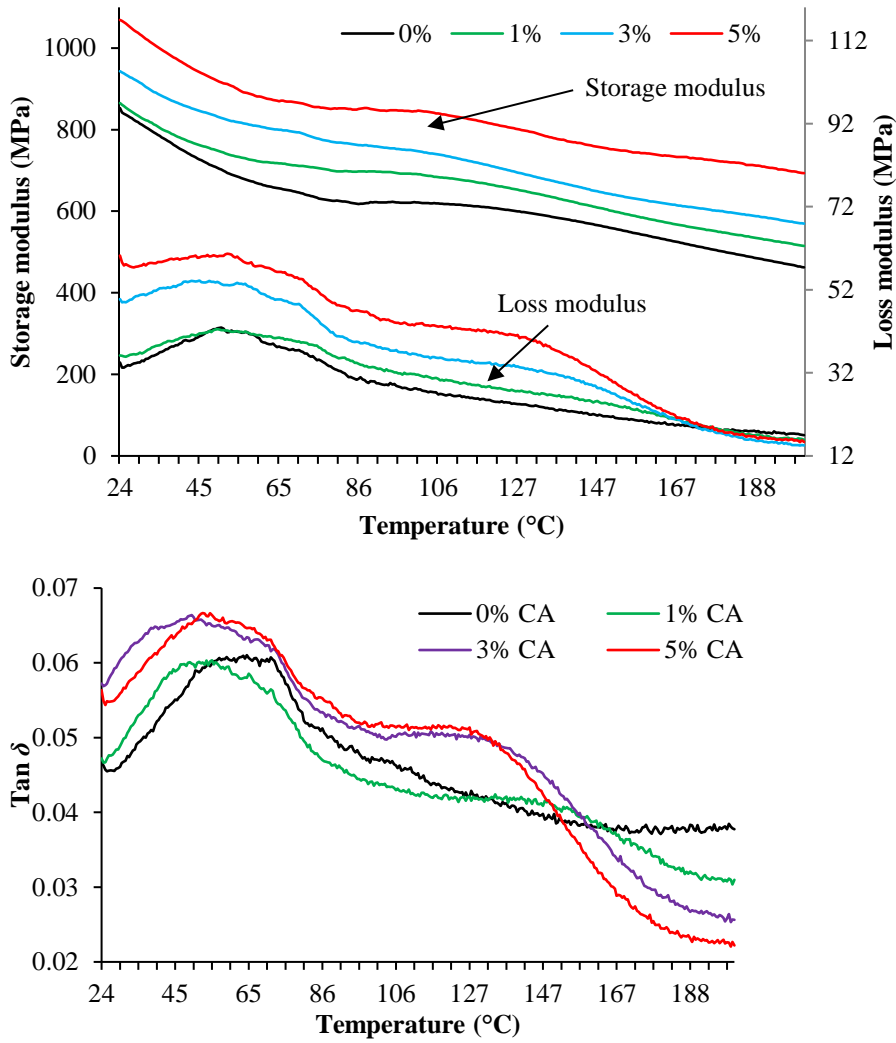


Fig. 4. Storage moduli and loss moduli (top) and $\text{Tan } \delta$ (bottom) at various temperatures of starch/cellulose composite foams cross-linked with various concentrations of citric acid as determined by DMTA.

In a viscoelastic system, $\text{Tan } \delta$ represents mechanical damping or internal friction, which is the ratio between the storage modulus and loss modulus. A high $\text{Tan } \delta$ value indicates that the material is viscous, and a low value indicates that the material is elastic. The effect of citric acid crosslinking on the mechanical loss factor, $\text{Tan } \delta$, is shown as a function of temperature in Fig. 4 (bottom). A sharp $\text{Tan } \delta$ peak indicates the glass transition temperature

(T_g) of the material, which is absent in the $\text{Tan } \delta$ curves of both control and the crosslinked composite foams. The control and the crosslinked composites showed broad peaks at around 60 °C, suggesting that they do not have any defined T_g . However, the citric acid-crosslinked starch/cellulose composites also showed a secondary broad peak at 135 to 150 °C associated with the formation of a crosslinked network. The height of the secondary peak increased with an increase in the concentration of citric acid suggesting an increase in the degree of crosslinking.

3.5. Thermal stability

Thermogravimetric analysis is a tool to ascertain the effect of crosslinking of cellulose and starch on the thermal stability of the starch/cellulose composites. The thermal stability of the starch/cellulose composites only slightly improved after crosslinking with citric acid and with an increase in the applied dosage of citric acid as shown in Fig. 5 (top). The weight loss of starch/cellulose composites increased with temperature.

The control starch/cellulose and starch/cellulose composites crosslinked with various concentrations of citric acid all showed a three-stage weight loss. The weight loss at the first stage from room temperature to 120 °C occurred mainly due to the loss of moisture absorbed by starch and cellulose as both the polymers are hydrophilic (Tian et al., 2011). The weight loss that occurred at this stage was quite low, which was approximately 7.9% for the control starch/cellulose composites. The weight loss at this stage for the starch/cellulose composites crosslinked with 1 and 3% (w/w) citric acid was 7.4 and 7.5 % respectively. Hardly any weight loss was observed from 120 to 259 °C. For all the starch/cellulose foam composite

samples, the highest weight loss occurred at the second stage. For the control foam, the highest weight loss (48.1%) occurred at 259 to 325 °C due to the degradation of cellulose and starch producing various volatiles including carbon dioxide and carbon monoxide (Šmkovic & Jakab, 2001). In the case of starch/cellulose composites crosslinked with 1% citric acid, the weight loss occurred between 278 to 326 °C was 39.8%, considerably lower compared to the weight loss occurred for the control starch/cellulose composite foam at this stage. For the starch/cellulose composite crosslinked with 3% citric acid, the weight loss occurred at this stage was 42.7%. The second highest weight loss occurred at the 3rd stage due to further degradation of the degraded components of starch and cellulose. The weight loss that occurred for the control starch/cellulose composites from 325 to 600 °C was another 21.5%. However, for the starch/cellulose composites crosslinked with 1 and 3% citric acid, the weight loss was 26.0 and 22.2% respectively. The ash content at 600 °C for the control was 12.32% but the corresponding value for the starch/cellulose composites containing 1 and 3% citric acid was 12.94 and 13.8% respectively.

Fig. 5 (bottom) shows the DTG curves of starch/cellulose composite foams crosslinked with various concentrations of citric acid. The maximum degradation of control starch/cellulose composite occurred at 318 °C but for the composites crosslinked with 1 and 3% citric acid, the maximum degradation temperature increased to 324 and 327 °C respectively. It can be concluded that the crosslinking of starch/cellulose composites with citric acid slightly improved its thermal stability.

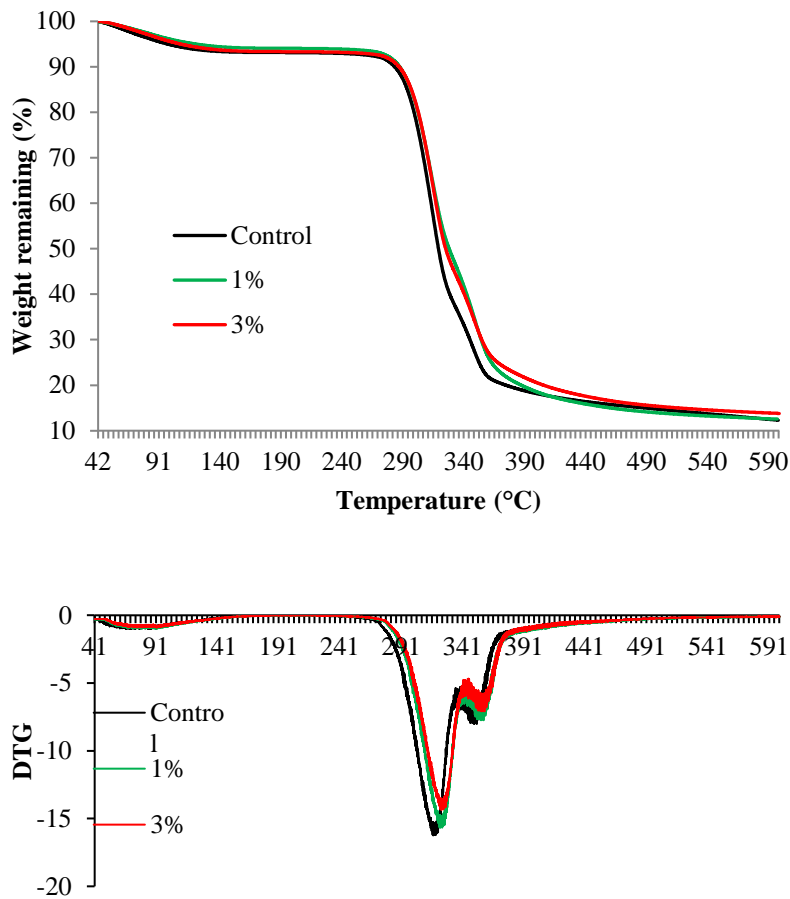


Fig. 5. Thermogravimetric (top) and DTG (bottom) curves of starch/cellulose composite foams crosslinked with 0, 1, and 3% (w/w) citric acid.

3.6. Water absorption

Cellulose and starch both are hydrophilic and therefore the composites made from them are hydrophilic. However, it is necessary to reduce the water absorbency of the composites to preserve their structural integrity when they are expected to be used in humid environments. As expected, the control starch-cellulose composite showed the highest water absorption capacity, but the composites crosslinked with citric acid showed considerably reduced water absorption compared to the control starch/cellulose composites as evident from Fig. 6.

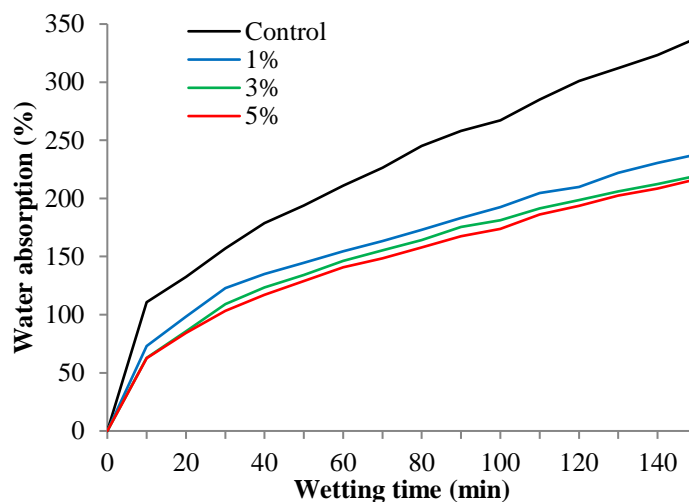


Fig. 6. Effect of citric acid concentration on the water absorption properties of starch/cellulose composite foam.

All composite foams, crosslinked or non-crosslinked, showed rapid absorption of water in the first 10 minutes, and after which the water absorption rate slowed down but gradually increased over the next 140 min. At 10 min of wetting time, the non-crosslinked control showed a 110.6% increase in weight. Conversely for the composites crosslinked with 1, 3, and 5% (w/w) citric acid the water absorption was 73.2, 62.9 and 62.6% respectively. After 150 min, the water absorption for the control sample reached 338.0% and the corresponding value for the composites crosslinked with 1, 3 and 5% (w/w) reached 237.9, 219.5 and 216.6% respectively. The water absorption shown by the starch/cellulose composites crosslinked with 5% (w/w) citric acid was marginally lower compared to the water absorption shown by the same composite crosslinked with 3% (w/w) citric acid. The crosslinking with citric acid blocked some of the hydroxyl groups of cellulose and starch resulting in decreased water absorption.

3.7. Dynamic contact angle and ATR-FTIR spectra

Table 2 shows the dynamic water contact angle of composites crosslinked with various concentrations of citric acid. The optical micrographs of water droplets placed on the starch/cellulose composite surface at various times are shown in Fig. S1 (Supplementary Material). The controlled starch/cellulose composite showed some level of hydrophobicity because of the presence of carnauba wax, but the contact angle gradually decreased with time showing that this hydrophobicity was not stable. The contact angle shown by the surface of non-crosslinked starch/cellulose foam at 0 s was 89.6°, which decreased to 79.4° after 480 s, consistent with our previous results (Hassan et al., 2019). The starch/cellulose composite crosslinked with 1% (w/w) citric acid had a contact angle that was stable over time. The contact angle shown by the composites crosslinked with 1% (w/w) citric acid at 0 s was 83.4°, which decreased to 82.3° at 480 s showing that the hydrophobicity exhibited by the crosslinked composites was quite stable.

Table 2

Dynamic contact angle of starch/cellulose foams composites crosslinked with 1, 3, and 5% (w/w) citric acid (numbers in the parenthesis are standard deviations based on five samples)

Citric acid concentrations (% w/w)	Average contact angle (°) at				
	0 s	120 s	240 s	360 s	480 s

0	89.6 (0.5)*	86.1 (0.9 *	82.6 (0.6 *	80.7 (0.9)	79.4 (0.9)
1	83.4 (0.4)*	83.2 (0.6)*	82.9 (0.5)*	82.6 (0.5)*	82.3 (0.4)*
3	96.2 (0.8)*	96.2 (0.7)*	96.4 (0.8)*	97.5 (0.4)	97.5 (0.7 *
5	102.1 (0.8)*	101.7 (0.5)*	101.2 (1.1)*	100.6 (0.8)	100.1 (0.9 *

* *p*-value less than 0.05

The contact angle increased with an increase in the concentration of the crosslinking agent and the contact angle was quite stable over 8 min of the test. The highest contact angle was shown by the composite crosslinked with 5% (w/w) citric acid, which showed a contact angle of 102.1° at 0 s, and decreased to 101.1° after 480 s. It is evident that the contact angle exhibited by the crosslinked composite foams was considerably higher than the contact angle observed for the control composite foam. The increase in hydrophobicity of the crosslinked composite foams observed by the increase in the contact angle with an increase in the citric acid concentration was further assessed by the ATR-FTIR spectral analysis.

Fig. 7 shows the ATR-FTIR spectra of control starch cellulose composite and starch/cellulose composites crosslinked with 3 and 5% (w/w) citric acid. The ATR-FTIR spectrum of non-crosslinked starch/cellulose composites shows characteristic IR bands of starch and cellulose at 758, 847, 930, 992, 1014, 1078, 1150, 1249, 2849, 2917, and

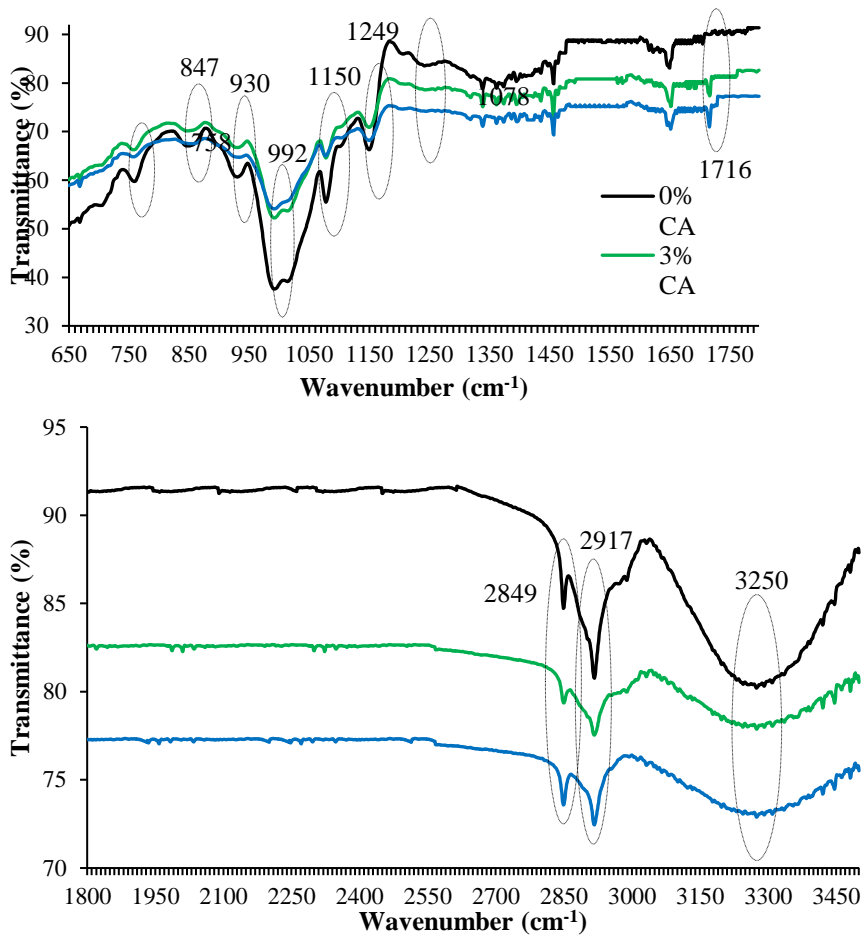


Fig. 7. ATR-FTIR spectra of starch/cellulose composite foams crosslinked with 0, 3, and 5% citric acid.

a broad band at 3255 cm^{-1} . The three characteristic bands that are shown between 980 and 1160 cm^{-1} (992 , 1014 , and 1078 cm^{-1}), could be assigned to the C–O bond stretching band attributed to primary alcohols (Marechal and Chanzy, 2000). The band at 1150 cm^{-1} can be assigned to the C–O–C asymmetric stretching vibrations, which shows that ether bonds were formed between the primary alcohol groups of starch resulting in a decrease in hydrophilicity. Therefore, the surface of the control starch/cellulose showed some level of hydrophobicity in the contact angle measurement (Table 2). Otherwise, it should be impossible to measure the contact angle of the control foam composite because of the strong hydrophilicity of cellulose

and starch. The bands at 2849 and 2917 cm^{-1} are due to symmetric and asymmetric C–H stretching vibrations. The broadband at 3255 cm^{-1} can be attributed to hydroxyl groups of starch and cellulose. The ATR-FTIR spectra of crosslinked starch/cellulose composites also showed similar bands except for a new band at 1716 cm^{-1} , which could be associated with the ester groups (Heredia-Guerrero et al., 2014). It is evident that the intensity of the ether band at 1150 cm^{-1} decreased with an increase in the concentration of citric acid but the intensity of the hydroxyl band at 3250 cm^{-1} considerably decreased with an increase in the concentration of citric acid suggesting that the hydrophilicity of the composites considerably decreased with an increase in the crosslinking of hydroxyl groups with citric acid. The results suggest that citric acid formed a cross-link between the hydroxyl groups of cellulose and starch, which decreased the moisture absorbing capacity of composite foams by blocking hydrophilic hydroxyl groups.

3.8. Surface morphologies

The fracture surfaces of the crosslinked composite foams were examined using scanning electron microscopy (SEM) to observe the effect of crosslinking on the microstructure of the composites. The control starch/cellulose composites showed quite different morphologies compared to the citric acid-crosslinked starch/cellulose composites (Fig. 8). The density of pores in the crosslinked composite was lower compared to the control composite foam. The top and bottom skin layers of all composites exhibited small, dense, and closed-cell foam structure, but the interior of the composite foams shows quite large and open cell structure. The size and distribution of the cells over the region are non-uniform. The dense outer skin layer was formed in the starch/cellulose batter layer adjacent to the hot surface of mould due

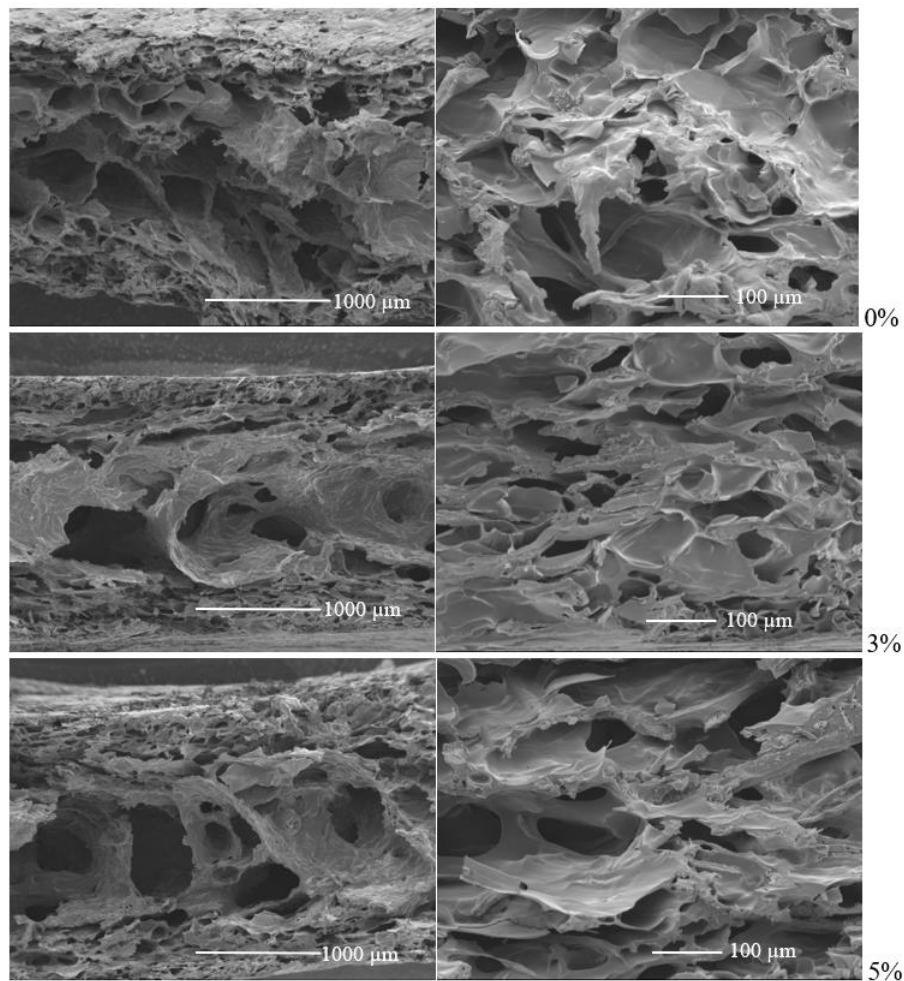


Fig. 7. SEM micrographs of the cracked surface of control starch/cellulose foam (a) and starch/cellulose composite foams crosslinked with 3% (b) and 5% (c) (w/w) citric acid.

to the obstruction of the evaporation of volatiles including water (Preechawong et al., 2005). It is also evident that in the case of crosslinked composites, the skin layers have more closed cells compared to the skin layers of the control composite foam. The citric acid crosslinking might have increased the starch/cellulose batter viscosity and changed the expansion behaviour and structure of the consequent foams produced. In the interior of the composite foams, the control starch/cellulose foam composite shows comparatively smaller and open

cells, but the crosslinked composites show larger pore with thicker cell walls compared to the control composite foam. In the interior of the composite foams, large opened cells were formed due to the rapid evaporation of a large amount of water during the high-temperature moulding, which expanded the pores before collapsing the pore walls during high-temperature moulding (Lawton et al., 1999). The control starch/cellulose composite foam showed a relatively uniform distribution of cells and uniform size of cells compared to the crosslinked starch/cellulose foam.

The neat surface of composite foams crosslinked with various concentrations of citric acid is shown in Fig. S2 (Supplementary Material). For all samples, cellulose fibres are visible on the surface of composite foams. SEM micrographs of control non-crosslinked starch/cellulose composite foams exhibit some non-gelatinised starch granules. It is evident that the spreading of starch increased with an increase in the concentration of citric acid and the crosslinked composite foams do not show any non-gelatinised starch granules on their surface. Citric acid is highly hygroscopic and binds water molecules, which slowed down the evaporation of moisture during crosslinking at 220 °C permitting starch granules to fully gelatinised and spread. In the case of the control sample, cellulose fibres did not form firm bonding with starch and gaps are visible between the cellulose fibre and starch matrix (Fig. S3 in Supplementary Material). However, in the case of crosslinked starch/cellulose composite foams, starch fully spread and firmly bonded with the cellulose fibres causing an increase in tensile strength as well as flexural strength.

Conclusions

Powdered cellulose fibres were mixed with moistened starch-containing citric acid and carnauba wax at room temperature by a low-shear food mixer, and crosslinked composite

foams were fabricated by compression moulding at 220 °C. The crosslinked composite foam showed better thermal stability, stiffness, tensile strength, flexural strength, and flexural modulus along with decreased water absorbency compared to a non-crosslinked control starch/cellulose composite foam. The maximum tensile strength, flexural strength, and storage modulus were shown by the composite foam crosslinked with 5% (w/w) citric acid but a further increase in the citric acid concentration resulted in a considerable decrease in those properties. The tensile strength exhibited by the composite foam crosslinked with 5% was 2.25 MPa compared to the exhibited by the non-crosslinked composite foam (1.76 MPa). Similarly, the flexural strength of non-crosslinked composite foam increased from 3.76 MPa to 7.61 MPa for the composite foam crosslinked with 5% citric acid. SEM images of the cracked surface of the foams reveal that the non-crosslinked foam had a higher number of open cells with thin cell walls, but the crosslinked foam showed a lower number of cells with thicker cell walls. These cross-linked starch/cellulose composite foams have the potential to replace expanded polystyrene foam packaging used for fruits and vegetables in supermarkets.

Acknowledgment

This work was financially supported by the Ministry of Business, Innovation, and Employment (MBIE) of the Government of New Zealand (Grant number BPLY1302) through the Biopolymer Network Ltd.

References

- Ali, A., Xie, F., Yu, L., Liu, H., Meng, L., Khalid, S., Chen, L. (2018). Preparation and characterisation of starch-based composite films reinforced by polysaccharide-based crystals. *Composites B* 133, 122–128.
- Avérous, L., Moro, L., Dole, P., Fringant, C. (2000). Properties of thermoplastic blends: starch-polycaprolactone. *Polymer*, 41, 4157–4167.
- Aygün, A., Uslu, M. K., Polat, S. (2017). Effects of starch sources and supplementary materials on starch based foam trays. *J. Polym. Environ.* 25, 1163–1174.
- Bergel, B. F., Dias Osorio, S., da Luz, L. M., Santana, R. M. C. (2018), Effects of hydrophobised starches on thermoplastic starch foams made from potato starch, *Carbohyd. Polym.* 200, 106–114.
- Chen, J., Long, Z., Wang, J., Wu, M., Wang, F., Wang, B., Lv, W. (2017). Preparation and properties of microcrystalline cellulose/hydroxypropyl starch composite films. *Cellulose* 24, 4449–4459.
- Cruz-Tirado, J. P., Vejarano, R., Tapia-Blácido, D. R., Barraza-Jáuregui, G., Siche, R. (2019). Biodegradable foam tray based on starches isolated from different Peruvian species. *Int. J. Biological Macromol.* 125, 800–807.
- Demitri, C., Del Sole, R., Scalera, F., Sannino, A., Vasapollo, G., Maffezzoli, A., Ambrosio, L., Nicolais, L. (2008). Novel superabsorbent cellulose-based hydrogels crosslinked with citric acid. *J. Appl. Polym. Sci.* 110, 2453–2460.
- Dos Santos, B. H., De Souza Do Prado, K., Jacinto, A.A., Da Silva Spinacé, M.A. (2018). Influence of sugarcane bagasse fibre size on biodegradable composites of thermoplastic starch. *J. Renew. Mater.* 6, 176–182.
- Edhirej, A., Sapuan, S.M., Jawaid, M., Zahari, N. I. (2017). Cassava/sugar palm fibre reinforced cassava starch hybrid composites: Physical, thermal and structural properties. *Int. J. Biological Macromol.* 101, 75–83.

- Ghosh Dastidar, T., Netravali, A. N. (2012). 'Green' crosslinking of native starches with malonic acid and their properties. *Carbohydr. Polym.* 90, 1620–1628.
- Glenn, G. M., Orts, W. J., Nobes, G. A. R., Gray, G. M. (2001). In situ laminating process for baked starch-based foams. *Ind. Crop. Prod.* 14, 125–134.
- Gonenc, I., Us, F. (2019). Effect of glutaraldehyde crosslinking on degree of substitution, thermal, structural, and physicochemical properties of corn starch. *Starch* 71, 1800046.
- Heredia-Guerrero, J. A., Benítez, J. J., Domínguez, E., Bayer, I. S., Cingolani, R., Athanassiou, A., Heredia, A. (2014). Infrared and Raman spectroscopic features of plant cuticles: A review. *Front. Plant Sci.* 5 (2014) 305.
- Hassan, M. M., Le Guen, M. J., Tucker, N., Parker, K. (2019). Thermo-mechanical, morphological and water absorption properties of thermoplastic starch/cellulose composite foams reinforced with PLA. *Cellulose* 26, 4463–4478.
- Ibrahim, H., Mehanny, S., Darwish, L., Farag, M. (2017). A comparative study on the mechanical and biodegradation characteristics of starch-based composites reinforced with different lignocellulosic fibres. *J. Polym. Environ.* 26, 1–14.
- Jansson, A., Järnström, L. (2005). Barrier and mechanical properties of modified starches. *Cellulose* 12, 423–433.
- Lawton, J. W., Shogren, R. L., Tiefenbacher, K. F. (1999). Effect of batter solids and starch type on the structure of baked starch foams. *Cereal Chem.* 76, 682–687.
- Liu, D., Dong, Y., Bhattacharyya, D., Sui, G. (2017). Novel sandwiched structures in starch/cellulose nanowhiskers (CNWs) composite films. *Compos. Commun.* 4, 5–9.
- Liu, X. -X., Wang, Y. -F., Yu, L., Tong, Z., Chen, L., Liu, H. -S., Li, X. (2013). Thermal degradation and stability of starch under different processing conditions. *Starch* 65, 48–60.

- Jiang, S. -J., Zhang, T., Song, Y., Qian, F., Tuo, Y. -F., Mu, G. -Q. (2019). Mechanical properties of whey protein concentrate based film improved by the coexistence of nanocrystalline cellulose and transglutaminase. *Int. J. Biol. Macromol.* 126, 1266–1272.
- Marechal, Y., Chanzy, H. (2000). The hydrogen bond network in I β cellulose as observed by infrared spectrometry. *J. Molecular Struc.* 523, 183–186.
- Meng, L., Liu, H., Yu, L., Duan, Q., Chen, L., Liu, F., Shao, Z., Shi, K., Lin, X. (2019). How water acting as both blowing agent and plasticizer affect on starch-based foam. *Ind. Crop. Prod.* 134, 43–49.
- Mi, F. -L., Shyu, S. -S., Peng, C. -K. (2005). Characterisation of ring-opening polymerisation of genipin and pH-dependent crosslinking reactions between chitosan and genipin. *J. Polym. Sci. A* 43, 1985-2000.
- Muneer, F., Andersson, M., Koch, K., Menzel, C., Hedenqvist, M. S., Gällstedt, M., Plivelic, T. S., Kuktaite, R. (2015). Nanostructural morphology of plasticised wheat gluten and modified potato starch composites: relationship to mechanical and barrier properties. *Biomacromolecules* 16, 695–705.
- Nashed, G., Rutgers, R. P. G., Sopade, P.A. (2003). The plasticisation effect of glycerol and water on the gelatinisation of wheat starch, *Starch* 55, 131–137.
- Noorbakhsh-Soltani, S. M., Zerafat, M. M., Sabbaghi, S. (2018). A comparative study of gelatin and starch-based nanocomposite films modified by nano-cellulose and chitosan for food packaging applications. *Carbohydr. Polym.* 189, 48–55.
- Phiriyawirut, M., Mekaroonluck, J., Hauyam, T., Kittilaksanon, A. (2016). Biomass-based foam from crosslinked tapioca starch/ polybutylene succinate blend. *J. Renew. Mater.* 4, 185–189.
- Pinenq, P., Winnik, M. A. (2000). Polymer diffusion and mechanical properties of films prepared from crosslinked latex particles. *J. Coat. Technol.* 72, 45-61.

- Preechawong, D., Peesan, M., Supaphol, P., Rujiravanit, R. (2005). Preparation and characterisation of starch/poly(L-lactic acid) hybrid foams. *Carbohydr. Polym.* 59, 329–337.
- Ramos, L. A., Frollini, E., Koschella, A., and Heinze, T. (2005). Benzylolation of cellulose in the solvent dimethylsulfoxide/tetrabutylammonium fluoride trihydrate. *Cellulose* 12, 607–619.
- Reedy, N., Yang, Y. (2010). Citric acid crosslinking of starch films, *Food Chem.* 118, 702–711.
- Report No. EPA530-F-18-004 (2018). Advancing Sustainable Materials Management: 2015 Fact Sheet, United States Environmental protection Agency, USA.
- Romero-Bastida, C. A., Tapia-Blácido, D. R., Méndez-Montealvo, G., Bello-Pérez, L. A., Velázquez, G., Alvarez-Ramirez, J. (2016). Effect of amylose content and nanoclay incorporation order in physicochemical properties of starch/montmorillonite composites. *Carbohydr. Polym.* 152, 351–360.
- Sagnelli, D., Kirkensgaard, J. J. K., Giosafatto, C. V. L., Ogrodowicz, N., Kruczał, K., Mikkelsen, M. S., Maigret, J. -E., Lourdin, D., Mortensen, K., Blennow, A. (2017). All-natural bio-plastics using starch-beta-glucan composites. *Carbohydr. Polym.* 172, 237–245.
- Seligra, P. G., Medina Jaramillo, C., Famá, L., Goyanes, S. (2016). Biodegradable and non-retrogradable eco-films based on starch-glycerol with citric acid as crosslinking agent. *Carbohydr. Polym.* 138, 66–74.
- Shaikh, M., Haider, S., Ali, T. M., Hasnain, A. (2019). Physical, thermal, mechanical and barrier properties of pearl millet starch films as affected by levels of acetylation and hydroxypropylation. *Int. J. Biological Macromol.* 124, 209–219.

- Šmkovic, I., Jakab, E. (2001). Thermogravimetry/mass spectrometry study of weakly basic starch-based ion exchanger. *Carbohydr. Polym.* 45, 53–59.
- Soares, S., Ricardo, N. M. P. S., Jones, S., Heatley, F. (2001). High temperature thermal degradation of cellulose in air studied using FTIR and ^1H and ^{13}C solid-state NMR. *Eur. Polym. J.* 37, 737–745.
- Stepito, R.F. (2006). Understanding the processing of thermoplastic starch. *Macromol. Sympos.* 245–246, 571–577.
- Swanson, C. L., Shogren, R. L., Fanta, G. F., Imam, S. H. (1993). Starch-plastic materials—Preparation, physical properties, and biodegradability (a review of recent USDA research). *J. Environ. Polym. Degrad.* 1, 155–166.
- Tian, Y., Li, Y., Xu., X., Jin, Z. (2011). Starch retrogradation studied by thermogravimetric analysis (TGA). *Carbohydr. Polym.* 84, 1165-1168.
- Wang, P., Chen, F., Zhang, H., Meng, W., Sun, Y., Liu, C. (2017). Large-scale preparation of jute-fibre-reinforced starch-based composites with high mechanical strength and optimised biodegradability. *Stärke* 69, 1700052.
- Xu, M., Bian, J., Han, C., Dong, L. (2016). Hydrophobic modification of polypropylene/starch blend foams through tailoring cell diameter for oil-spill cleanup. *RSC Adv.* 6, 82088–82095.
- Zamudio-Flores, P. B., Torres, A. V., Salgado-Delgado, R., Bello-Pérez, L. A. (2010). Influence of the oxidation and acetylation of banana starch on the mechanical and water barrier properties of modified starch and modified starch/chitosan blend films. *J. Appl. Polym. Sci.* 115, 991–998.
- Zhou, J., Tong, J., Su, X., Ren, L. (2016). Hydrophobic starch nanocrystals preparations through crosslinking modification using citric acid. *Int. J. Biological Macromol.* 91, 1186–1193.

